Microstructural analysis of asphalt mixtures containing recycled asphalt materials using digital image processing

Augusto Cannone Falchetto[1, a], Ki Hoon Moon[2, b], Michael P. Wistuba[1, c]

[1] *Department of Civil Engineering, Technische Universität Braunschweig, Braunschweig, Germany*
[2] *Material R&D Division, Samsung Corporation, Seoul, South Korea*

[a] a.cannone-falchetto@tu-bs.de
[b] zetamkh@ex.co.kr
[c] m.wistuba@tu-bs.de

Digital Object Identifier (DOI): dx.doi.org/10.14311/EE.2016.195

ABSTRACT

The use of recycled materials in pavement construction has seen, over the years, a significant increase closely associated to substantial economic benefits and to the demand of environmentally friendly constructions materials which limit the intensive exploitation of natural resources. Over the past decades, the use of different types of recyclable materials such as Reclaimed Asphalt Pavement (RAP) has been considered. However, most research efforts investigating the effect of adding recycled asphalt materials in asphalt paving mixtures were focused on experimental testing and performance evaluation, while the effect on asphalt mixtures microstructure has only recently seen increased attention. In this paper, the effect of adding RAP on the microstructural properties of asphalt mixtures is investigated using digital image processing (DIP) of digitalized images acquired by scanning Bending Beam Rheometer (BBR) specimens made of asphalt mixture. Detailed information on the internal microstructure is obtained from Red Green and Blue (RGB) images of small BBR beams and based on three-phase material analysis (aggregate, asphalt mastic and air voids). The numerical estimations of the spatial correlation functions and of the corresponding autocorrelation length (ACL) are then performed to quantitatively determine the impact of the recycled material on spatial distribution of the three mixture phases. The microstructural distributions of aggregates, asphalt mastic, and air voids were not significantly affected by the addition of RAP up to 40%. However, an increase in Auto Correlation Length (ACL) was found for RAP mixtures in comparison with conventional mixtures. The proposed DIP analysis method has the potential of being used as a forensic quality control tool to verify if the mixing process affects the microstructural distribution of the asphalt mixture constituents potentially resulting in poor mechanical performance.

Keywords: Aggregate, Creep, Reclaimed asphalt pavement (RAP) Recycling, Voids

1. INTRODUCTION

Using recycled materials is commonly accepted for reducing construction budget and environmental pollution in the asphalt pavement industry. The use of Reclaimed Asphalt Pavement (RAP) has been documented for more than three decades, indicating that RAP is the most recycled material in U.S. [1]. However, the addition of RAP may have a detrimental effect on the mechanical properties of asphalt mixtures due to the oxidized bitumen. Therefore, some road authorities have limited the use of RAP to specific percentages [2].

Most of the research efforts investigating the effect of adding RAP on asphalt mixtures focused on experimental work and performance evaluation [1-3]. However, the microstructure of RAP mixture as described by the spatial distribution of its components, aggregate, asphalt mastic (and/or bitumen) and air voids, has found limited attention, although Digital Image Processing (DIP) has been used to model conventional asphalt mixtures.

DIP analysis was used in the past [4] and more recently to address the microstructural properties and to reconstruct the geometry of asphalt mixture for advanced numerical simulations [5]. A number of authors [6, 7] have also proposed different analysis techniques based on 3D X-Ray Computer Tomography (CT) technology.

The microstructural information obtained with DIP techniques can be also used together with high-order microstructure functions, such as *n*-point correlation functions, to obtain information on the mechanical material properties of the material [8]. It is well known that the spatial distribution of the constituents of a composite material can significantly influence its mechanical properties [8]. In the recent past simplified approaches were used to evaluate the distribution of the asphalt mixture phases and to estimate the representative volume elements [9]; nevertheless, a robust and practical solution is needed to evaluate the influence of recycled materials in the mixture.

2. OBJECTIVE AND RESEARCH APPROACH

In this paper, 2D scanned Red Green Blue (RGB) scale images of asphalt mixture and advanced DIP analyses are used in combination with higher order statistical functions, such as 2- ad 3- point correlation functions, with the objective of investigating the effect of adding different amounts of RAP on the microstructure of asphalt mixtures. To achieve such a goal, the following research approach was conceived:

- Obtain extensive information on aggregate, asphalt mastic and air voids structure of asphalt mixture beam specimens, based on simple digital scanning.
- Determine a 2D three-phase (aggregate, asphalt mastic and air voids) representation of asphalt mixture using DIP techniques.
- Estimate 2- and 3-point correlation functions of the three material phases.
- Calculate and compare the values of Auto Correlation Length (ACL) of the material phases.

3. MATERIAL AND PREPARATION OF SPECIMENS

Twelve mixtures, prepared and compacted in the asphalt pavement laboratory at University of Minnesota were used in this study (Table 1) [10].

Table 1: Asphalt mixtures

ID	Group	Bitumen	Target Air Voids (%)	RAP (%)	*VMA* (%)	V_{air} (%)	V_{mastic} (%)	NMAS (mm)
1		PG		40%	16.37	6.10	10.27	19.0
2	1	58-28	7%	25%	17.15	6.53	10.62	19.0
3		Plain		0%	17.52	6.91	10.61	12.5
4		PG		40%	14.01	3.45	10.56	19.0
5	2	58-28	4%	25%	14.50	3.54	10.96	19.0
6		Plain		0%	15.69	4.85	10.84	12.5
7		PG		40%	16.91	6.10	10.81	19.0
8	3	58-34	7%	25%	17.35	6.45	10.90	19.0
9		Modified		0%	17.41	6.79	10.62	12.5
10		PG		40%	14.23	3.08	11.16	19.0
11	4	58-34	4%	25%	15.20	4.02	11.18	19.0
12		Modified		0%	15.65	4.80	10.85	12.5

* *VMA*: Voids in the Mineral Aggregate, NMAS: Nominal Maximum Aggregate Size

* Air voids (%): means target value

* V_{air} and V_{mastic} (%) were measured in the laboratory

The mixtures were prepared using a PG58-28 unmodified bitumen and PG58-34 polymer modified bitumen, two air voids levels (4% and 7%), and three RAP contents (0%, 25%, and 40%). Asphalt cylindrical samples were prepared with a Superpave Gyratory Compactor (SGC) and five mixture slices, with the radius of 75.0±10.0mm and thickness of 12.7±0.5mm, were cut from each cylinder. Then, from each slice, ten asphalt mixture beams with dimensions of 102±10.0mm × 12.7±0.5mm × 6.35±0.5mm (the specimen size for BBR mixture creep testing [11]), were cut to

generate 2D three-phase asphalt images. For DIP analysis, all beam sides: top, bottom, right and left, were used. For 2- and 3-point correlation function estimation, only the top and bottom sides (102±10.0mm×12.7±0.5mm) were considered.

4. IMAGE ANALYSIS OF ASPHALT MIXTURE

4.1 Digital image processing: overview

The internal structure of random heterogeneous materials, such as asphalt, can be described as a two dimensional independent function, $f(x, y)$, where f indicates the function of color intensity and x and y are the coordinate of the specific pixel in the image [12]. In the present research, a flat-bed scanner was used to obtain 2D images of asphalt in RGB format. The resolution was limited to 720dpi since this is sufficient to detect filler particles (75μm). Then, MATLAB™ [13] was used to convert RGB images of asphalt into 8 bit gray-scale images having color intensity from 0 (black) to 255 (white) with reduced noise levels (Figure 1).

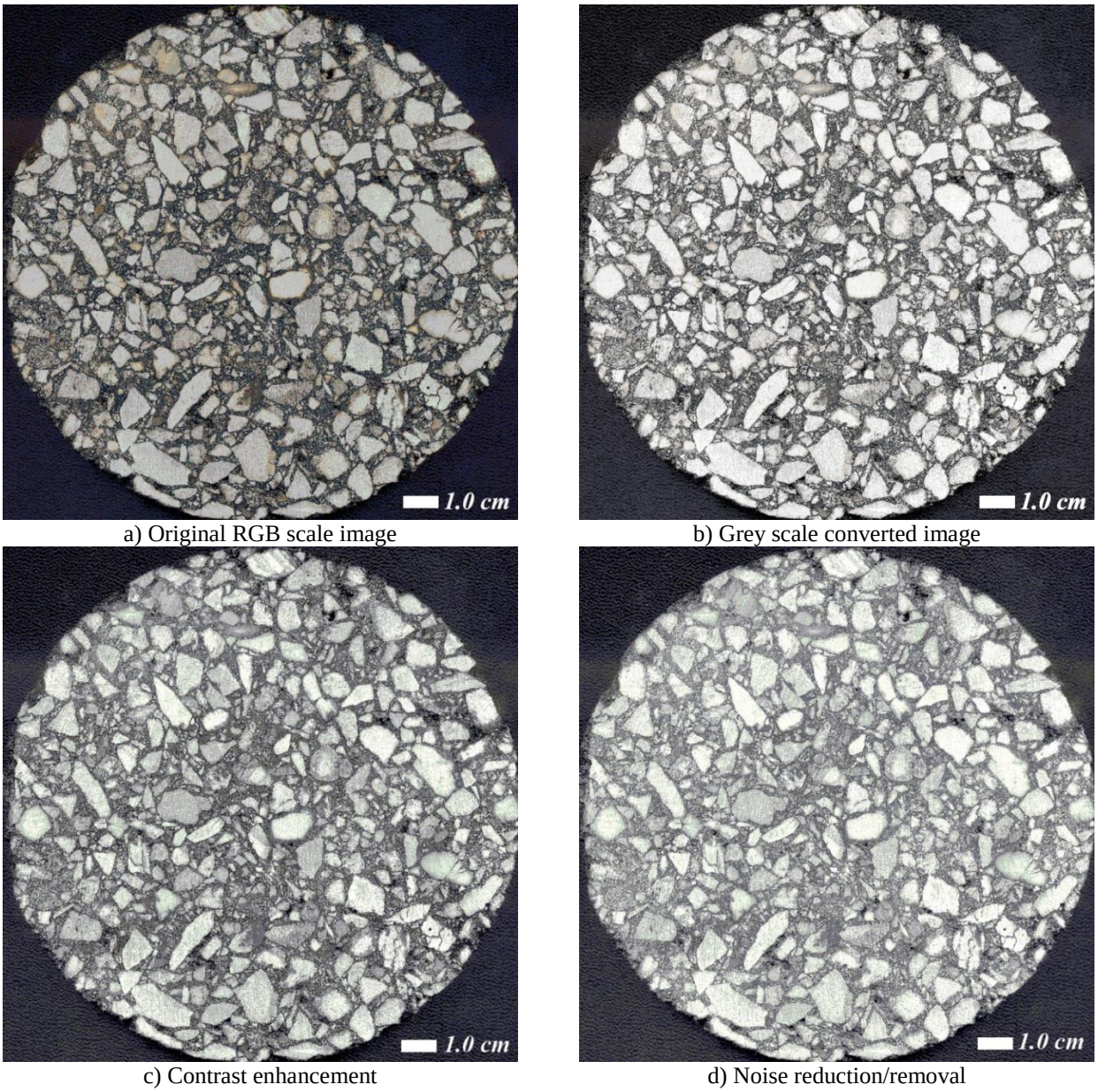

a) Original RGB scale image

b) Grey scale converted image

c) Contrast enhancement

d) Noise reduction/removal

Figure 1: DIP analysis of asphalt slices (Mixture 1)

Three-phase asphalt mixture images, accounting for aggregate, asphalt mastic and air voids, were generated using the values of the Voids in the Mineral Aggregate (VMA) and a series of DIP steps including global thresholding [9]. This technique was applied to asphalt slices (3,540 × 3,540 pixels) and to 600 (=12×5×10) asphalt mixture BBR beams [11] obtained from the mixture slices. Based on this process two threshold level, T_1 and T_2, corresponding to air voids and asphalt mastic, respectively, were identified and used to finally generate the three-phase asphalt representations.

4.2 Threshold computation for air voids and asphalt mastic: T_1 and T_2

In the recent past, a number of threshold algorithms for the segmentation of aggregate, asphalt mastic and air voids were proposed [7, 9 and 14]. In this study simple DIP analysis and volumetric data, were used to generate three-phase asphalt images. A total five asphalt slices were prepared from each mixture set [6, 10]. The following procedure was prepared for computing the two threshold values, T_1 and T_2:

- In the digital image (gray scale) of asphalt, the air voids component was assumed to take the darkest part in the color intensity range. Therefore, the threshold value for air voids, T_1, was computed in the range from 0 to T_1 ($0<T_1<255$) based on the volume fraction of air voids, V_{air}, experimentally obtained (Table 1). For example, for Mixture 1, V_{air}=6.10%. Using this value, the implemented MATLAB™ code can find the maximum color intensity number T_1 for which air voids take approximately 6.10% of the entire image.
- Similarly, the threshold value of asphalt mastic, T_2, was obtained in a range from 0 to T_2 ($0<T_1<T_2<255$) based on the results of VMA (Table 1). Then, the volume fraction of asphalt mastic was calculated as $V_{mastic}=V_{T2}-V_{T1}$.

It should be mentioned that because of the irregular wall surface of the SGC asphalt cylinder and to avoid misleading results on air voids, images with reduced slice radius (radius-5mm) were used for computing the two threshold values T_1 and T_2. Table 2 list the computed average threshold values, while an example of three-phase asphalt slice images are presented in Figures 2. In Table 2, the low values of the Coefficient of Variation (CoV<10%, max=7.45%) provide evidence that the asphalt slices present similar volume fractions of aggregate, asphalt mastic and air voids.

Table 2: Threshold values

ID	Group	Bitumen type	T_1		T_2	
			Ave	CoV (%)	Ave	CoV (%)
1	1	PG 54-28 Plain	92	3.22	116	1.63
2			89	4.14	119	1.41
3			99	1.70	125	1.27
4	2	PG 54-28 Plain	82	2.51	111	1.74
5			80	7.45	110	1.88
6			91	4.18	123	1.57
7	3	PG 54-34 Modified	92	1.37	118	1.79
8			92	1.38	117	1.44
9			100	0.00	124	0.00
10	4	PG 54-34 Modified	80	1.59	109	1.77
11			84	0.00	112	0.00
12			90	2.28	119	1.41

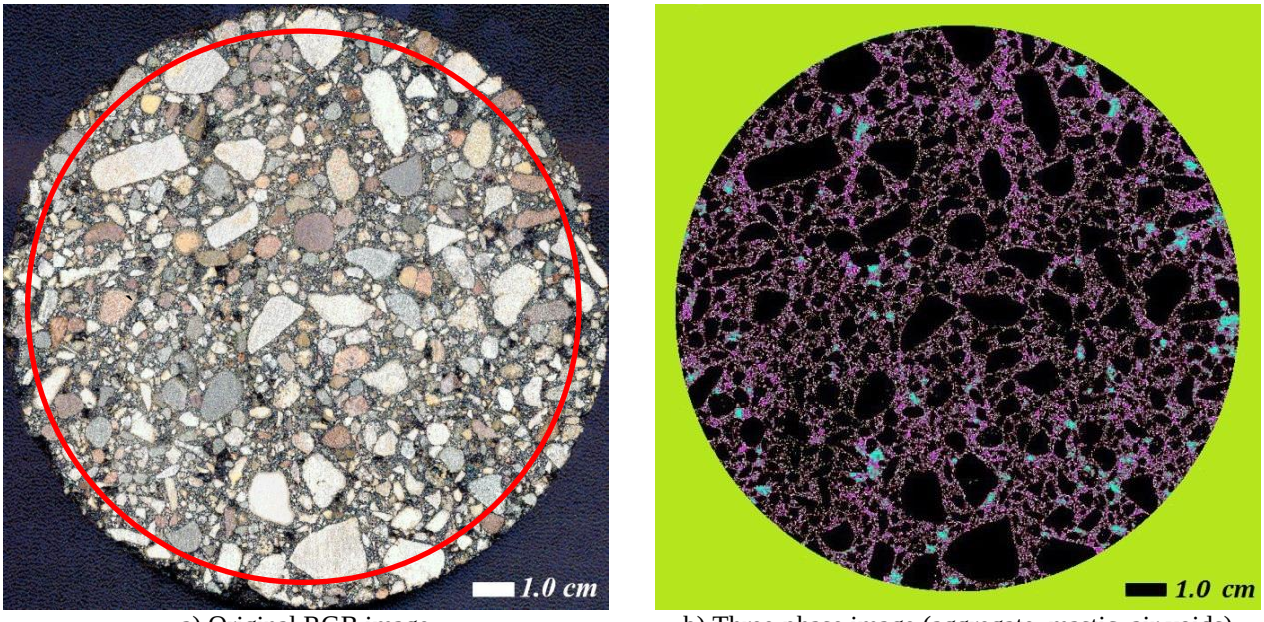

a) Original RGB image b) Three-phase image (aggregate, mastic, air voids)

Figure 2: Three-phase representation of Mixture 2.

In the generated three-phase images shown in Figure 2 (right picture), the green color represents the background, the cyan color indicates air voids, the violet color corresponds to asphalt mastic and the black color denotes the aggregates

(bigger than 75μm); a red circle in the RGB scale image (left picture) defines the portion of image used in the DIP analysis.

4.3 Three-phase representation of asphalt beams

A three-step procedure was followed to generate three-phase asphalt beam images (2600×294×147pixels) through DIP:

- From the asphalt slices, 600 asphalt beams were cut and a total of 2400 (=12×5×10×4) images were used for DIP analysis.
- First, the threshold T_1 was applied to the gray-scale converted image to generate the air voids phase; all the pixels with a value lower or equal to T_1 ($T \leq T_1$) were converted into cyan color indicating the air voids.
- Then, the second threshold T_2 was used to identify asphalt mastic. All the pixels with color intensity, T, in the interval $T_1 < T \leq T_2$ were converted into violet color indicating asphalt mastic.

Table 3 shows the computed results of the average VMA_d, V_{air_d} and V_{mastic_d} for the three-phase asphalt beam images (Figure 3).

Table 3: Volumetric parameters of asphalt beams obtained through DIP

ID	Group	RAP (%)	VMA_d (%)		V_{air_d} (%)		V_{mastic_d} (%)		VMA* (%)	V_{air}^* (%)	V_{mastic}^* (%)
			Ave	CoV	Ave	CoV	Ave	CoV			
1	1	40	15.97	5.16	8.43	4.59	7.54	7.84	0.40	2.33	-2.73
2		25	17.00	6.08	7.58	2.01	9.42	9.68	0.15	1.05	-1.20
3		0	17.49	6.83	6.67	7.05	10.82	9.16	0.03	-0.24	0.21
4	2	40	14.10	6.65	6.04	10.86	8.06	4.79	0.09	2.59	-2.50
5		25	14.13	6.92	4.99	4.95	9.14	12.47	0.38	1.45	-1.82
6		0	15.83	3.57	4.66	5.37	11.17	6.99	0.15	-0.19	0.33
7	3	40	17.02	5.41	8.65	7.94	8.37	5.67	0.11	2.55	-2.44
8		25	16.84	2.19	7.05	6.20	9.79	3.93	0.51	0.60	-1.11
9		0	17.66	3.56	6.73	1.93	10.93	5.32	0.24	-0.06	0.31
10	4	40	14.72	4.94	5.87	6.48	8.85	8.40	0.47	2.79	-2.31
11		25	15.07	1.35	4.92	12.69	10.15	5.92	0.13	0.90	-1.03
12		0	15.49	5.40	4.41	10.33	11.08	5.39	0.16	-0.39	0.23

*$VMA^* = (VMA - VMA_d)$, $V_{air}^* = (V_{air} - V_{air\_d})$, $V_{mastic}^* = (V_{mastic} - V_{mastic\text{-}d})$

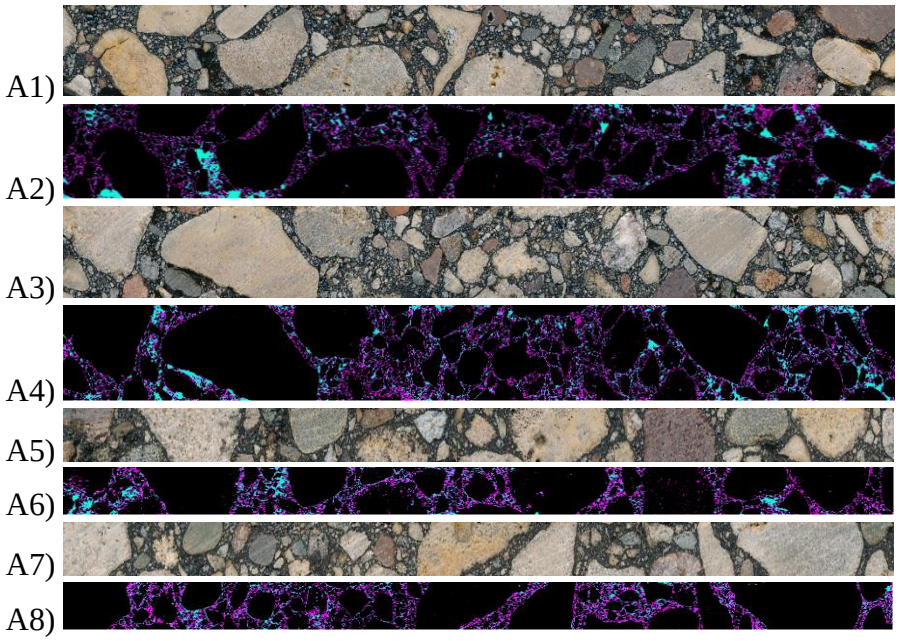

Figure 3: RGB and three-phase representation of an asphalt beam - Mixture 5

The use of volumetric parameters for generating three-phase images of asphalt beams provides accurate visual images in comparison with the original RGB images. Table 3 indicates that for conventional asphalt (mixtures 3, 6, 9, 12), similar VMA_d, V_{air_d} and V_{mastic_d} can be found in the generated three-phase images in comparison with the experimental VMA , V_{air} and V_{mastic} (Table 1). However, for RAP mixtures, a similar VMA_d was observed, while V_{air_d} and V_{mastic_d} were either overestimated or underestimated depending on the measured values of V_{air} and V_{mastic}, respectively (about

±1.1% for RAP 25% and ±2.5% for RAP 40% mixtures). This can be explained with the darker color of the RAP aged bitumen which is only partially blended with the virgin bitumen. This does not affect VMA_d, but only V_{air_d} and V_{mastic_d} with larger error for higher RAP amounts. Similarly to the asphalt slices, low CoV (max=12.5%) were observed suggesting that the asphalt beams have similar volume fraction of aggregate, asphalt mastic and air voids even though larger differences would be expected when considering smaller material quantity as in the case of BBR specimens. Therefore, it appears that the proposed DIP technique can be also potentially used to generate detailed geometry for numerical simulations such as Finite Element Method (FEM) and Discrete Element Method (DEM).

5. NUMERICAL ESTIMATION OF CORRELATION FUNCTIONS

5.1 *n*-point correlation function

Correlation functions provide statistical information on how much different points in a material, located at specific positions affect each other. In case of random heterogeneous materials, higher-order microstructural information is critical for understanding the material behavior and several functions, such as the *n*-point correlation functions and surface correlation functions, can be used for such a purpose. Among these functions, the 2- and 3-point correlation functions are selected because of their simplicity [15-18].

The *n*-point spatial correlation function measures the probability of finding all *n* points located on the space occupied by one of the phases of a heterogeneous material [16]. For instance, the 1-point correlation function, S_1, measures the probability that any point lies on phase 1 and this corresponds to the volumetric fraction of phase 1. The 2-point correlation function, S_2, calculates the probability that two points separated by a certain distance are located both in the same phase. Similarly, the 3-point correlation function, S_3, computes the probability that all the vertices of one triangle are located in the same phase.

The *n*-point correlation functions of a two-phase random heterogeneous material in a *d*-dimensional Euclidian space, R_d, were defined as [17]:

$$S_n^{(i)}(x_1, x_2, x_3, ..., x_n) = \left\langle I^{(i)}(x_1) I^{(i)}(x_2) I^{(i)}(x_3) \cdots I^{(i)}(x_n) \right\rangle \quad (1)$$

where $\langle\ \rangle$ is the ensemble averaging and $I^{(i)}(x)$ is the indicator function.

The *n*-point correlation function shows a translationally invariant characteristic for a statistically homogeneous material. Therefore, the function depends on the differences in the coordinate values of the x_i vectors [17] and, hence, the origin of the coordinate system is not an important factor. The *n*-point correlation function can also be expressed as:

$$S_n^{(i)}(x_1, x_2, x_3, ..., x_n) = S_n^{(i)}(x_{12}, x_{13}, x_{14}, ..., x_{1n}) \quad (2)$$

where $x_{ij} = x_j - x_i$ is the difference between the two vectors x_j and x_j, and x_1 is the selected reference vector.

The 1-point correlation function represents the volume fraction ϕ_i of the selected i^{th} phase, is constant and it is the probability that a randomly selected point in the whole matrix belongs to i^{th} phase:

$$S_1^{(i)} = \left\langle I^{(i)}(x) \right\rangle = \phi_i \quad (3)$$

The 2- and 3-point correlation function can be defined, respectively as [17]:

$$S_2^{(i)}(x_1, x_2) = \left\langle I^{(i)}(x_1) I^{(i)}(x_2) \right\rangle \quad (4)$$

$$S_3^{(i)}(x_1, x_2, x_3) = \left\langle I^{(i)}(x_1) I^{(i)}(x_2) I^{(i)}(x_3) \right\rangle \quad (5)$$

If the material contains a translationally invariant isotropic characteristic, the 3-point correlation function can also be written as:

$$S_3^{(i)}(r_1, r_2) = S_3^{(i)}(|r_1|, |r_2|, u_{12}) \quad (6)$$

where $r_1 = x_2 - x_1$ and $r_2 = x_3 - x_1$ are vectors, and u_{12} is the cosine of the angle θ_{12} between vectors r_1 and r_2. If the microstructure of the material does not present long range order, the initial value of 2- and 3-point correlation function is ϕ_i (r=0), while, for very large r ($r \to \infty$), it reaches the asymptotic limits of ϕ_i^2 and ϕ_i^3, respectively.

The *n*-point correlation function can describe the microstructure of random heterogeneous materials such as asphalt mixtures; however, the computation process is complicated and, therefore, a convenient numerical solution is needed [17].

5.2 Numerical approach to the 2-point correlation function

In the past a discretized version of the 2-point correlation function which can estimate S_2 from digital image of size M×N pixels was proposed [17]. However, this solution was found to require large or, sometimes, prohibitive computation times for high resolution images. Therefore, a simplified computation algorithm [9,11] based on Monte Carlo simulation and on a simple MATLAB™ [13] code was used in this study. Figure 4 shows the schematic of the 2-point correlation function computation.

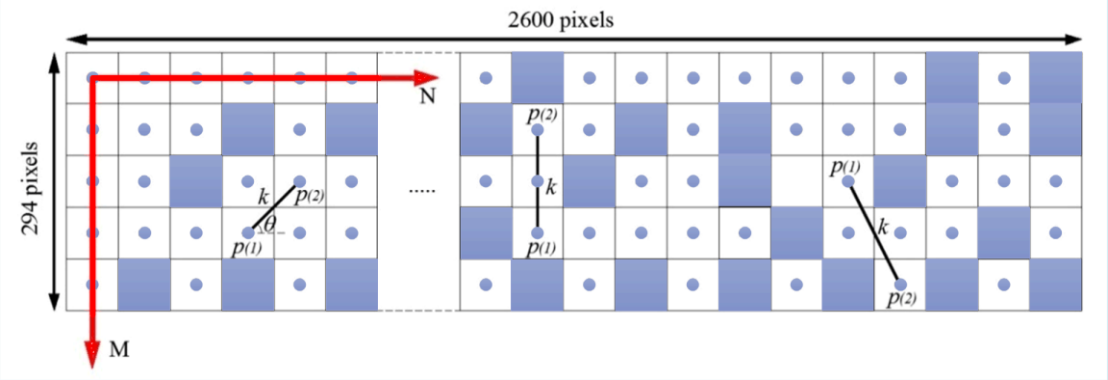

Figure 4: Schematic of 2-point correlation function calculation

First, two random points p_1 and p_2, are generated; the two points are the end points of a segment of length k which forms a randomly generated angle θ with the horizontal line. The points are iteratively generated and the number of hits for which the two points are located in the same phase (aggregate, asphalt mastic or air voids), $N_{k\text{-}hits}$, is recorded for each k, respectively. Finally the 2-point correlation function is computed as:

$$S_2(k, p_1, p_2) = \frac{N_{k\_hits}}{N_{total}} \tag{7}$$

where N_{total} is the total number of drops at each k. Based on previous research [9], N_{total} in the order of 100,000 was used to obtain reliable results. To further reduce computation time from 3 hours to 2 minutes per calculation, the value of k was limited within a range 0 to M/2.5 (5mm) [9, 19].

In total, 15 top and bottom sides of each three-phase asphalt mixture beam images (2600×294 pixels corresponding to 102×12.7 mm), were randomly selected per each mixture set to run the 2-point correlation function simulations. The summaries of the 2-point correlation computation of the aggregate phase results are listed in Table 4. Figure 5 present the curves of average 2-point correlation function for all four groups of asphalt mixtures (Table 1).

Table 4: 2-point correlation function values comparison (Aggregate phase)

ID	Group	S_1	S_2 at k = 5mm	S_2 theoretical	Error at k = 5mm	CoV max (%)
1		0.840	0.712	0.706	0.75%	4.75%
2	1	0.829	0.693	0.687	0.59%	4.47%
3		0.825	0.698	0.681	2.45%	3.23%
4		0.859	0.741	0.738	0.48%	3.49%
5	2	0.858	0.739	0.738	0.18%	2.78%
6		0.841	0.713	0.708	0.71%	2.15%
7		0.829	0.690	0.689	0.23%	4.59%
8	3	0.831	0.683	0.692	1.25%	3.86%
9		0.823	0.674	0.678	0.56%	3.39%
10		0.852	0.720	0.727	0.99%	4.40%
11	4	0.849	0.723	0.721	0.17%	3.32%
12		0.845	0.702	0.714	1.69%	4.80%

* S_1: Volume fraction of aggregate phase

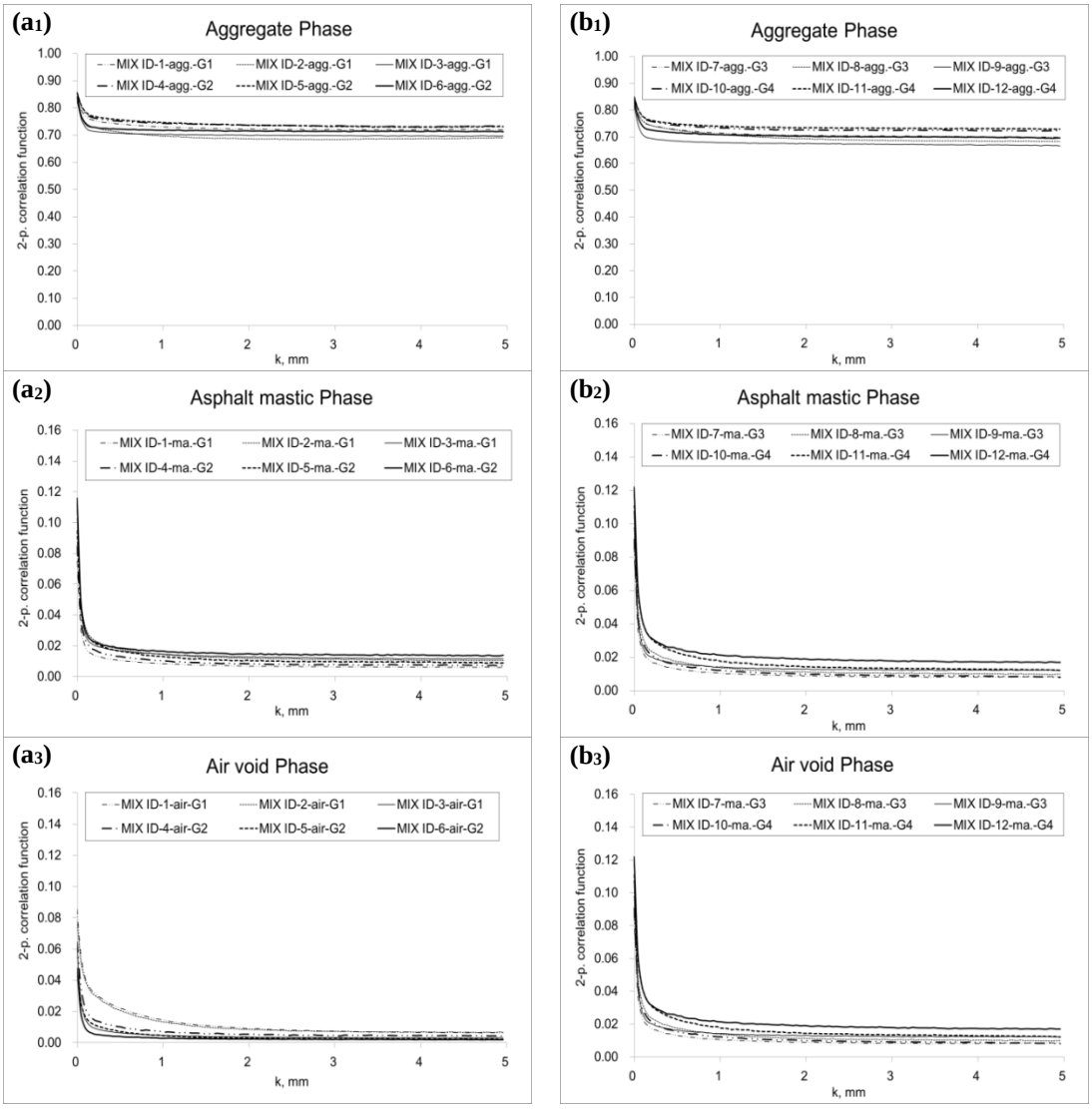

Figure 5: 2-point correlation function for mixture Groups 1 to 4

All the tested mixtures (including RAP mixtures) showed similar behavior: the values of the 2-point correlation function did not fluctuate with the increase of distance, *k*. The functions starts at S_1 ($\phi_{aggregate}, \phi_{mastic}$ and $\phi_{air\text{-}void}$) and then, after *k* increases, smoothly drops approximately to S_1^2 ($\phi^2_{aggregate}, \phi^2_{mastic}$ and $\phi^2_{air\text{-}void}$) $\cong S_2$. This indicates that no significant differences in the microstructure were found up to 40% of RAP content. It can be also observed that low errors (max=2.45% for Mixture 3, aggregate phase) and CoV (max=4.80% for Mixture 12, aggregate phase) were detected, which indicates good results repeatability.

5.3 Numerical approach to the 3-point correlation function

The 2-point correlation function can provide non trivial information about the material properties based on its microstructure. However, when clustering and/or connected path has to be investigated, higher order microstructural information can be obtained using 3-point correlation function [8]. Similarly to the 2-point correlation function, the use of brute-force method is highly discouraged. To calculate 3-point correlation function, a method using a set of symmetric triangles based on the Monte Carlo simulation [16] was applied. Figure 6 shows the schematic of 3-point correlation function computation used in this paper.

For an isotropic and statistically homogeneous material only size and shape of triangle have significant effect in 3-point correlation computation. The sets of triangle used for the calculation of 3-point correlation functions are defined by three integers: *l*, *m* and *n* (Figure 6) which are related by the following conditions:

a) $m \le l/2$ b) $m^2 + n^2 \le 2ml$ c) $2m = 2n = l$ (8)

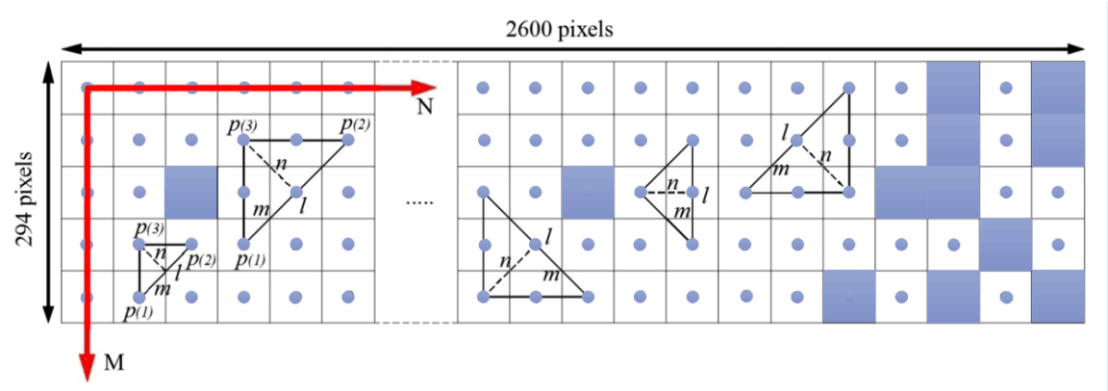

Figure 6: Schematic of 3-point correlation function calculation

In this study, the triangles of the same symmetric shape and having different sizes (0mm < l ≤ 5.2mm) were used. This restricted analyses cannot fully validate the entire computation of 3-point correlation functions, but this method can reduce the computing time from 4~5 hours to 2~3 minutes per each simulation [9] still providing important information. Similarly to the 2-point correlation function, top and bottom surfaces of three-phase asphalt beam images were used. A MATLAB™ [13] code was written for the 3-point correlation function. Each triangle defined by the integer coordinate, (*l*, *m*, *n*), was dropped in the generated three-phase asphalt image. Then, the number of hits, N_{l_hits}, was counted when all the three points were dropped in the same phase. A total of 100,000 vector drops, N_{drops}, were applied to each triangle length, *l*. Finally, the 3-point correlation functions for the aggregate, asphalt mastic and air-voids phase were computed as:

$$S_3(l,m,n) = \frac{N_{k\_hits}}{N_{drop}} \tag{9}$$

The summary of the 3-point correlation computation of the aggregate phase is listed in Table 5. Figure 7 presents the curves of average 3-point function estimation for all four groups of estimated asphalt listed in Table 1.

Table 5: 3-point correlation function values - Aggregate phase

ID	Group	S_1	S_3 at l = 5.2mm	S_3 theoretical	Error at l = 5.2mm	CoV max (%)
1		0.840	0.612	0.594	3.00%	5.94%
2	1	0.829	0.570	0.572	0.20%	5.26%
3		0.825	0.568	0.562	1.08%	3.20%
4		0.859	0.643	0.634	1.41%	4.55%
5	2	0.858	0.641	0.633	1.14%	5.24%
6		0.841	0.595	0.596	0.15%	3.42%
7		0.829	0.575	0.571	0.56%	5.91%
8	3	0.831	0.581	0.575	1.00%	4.75%
9		0.823	0.557	0.558	0.18%	4.47%
10		0.852	0.622	0.620	0.28%	6.28%
11	4	0.849	0.624	0.613	1.84%	4.49%
12		0.845	0.590	0.604	2.27%	5.19%

The 3-point correlation function did not fluctuate with the increase of *l* showing low CoV (max=6.28% for Mixture 10, aggregate phase). The function initial value was S_1 ($\phi_{aggregate}$, ϕ_{mastic} and $\phi_{air\text{-}void}$) and, after *l* increases, it dropped approximately to S_1^3 ($\phi^3_{aggregate}$, ϕ^3_{mastic} and $\phi^3_{air\text{-}void}$)) ≅ S_3, similarly to the theoretical results of 2-point correlation function. Therefore, no clustering and/or connected paths were detected up to 40% RAP content.

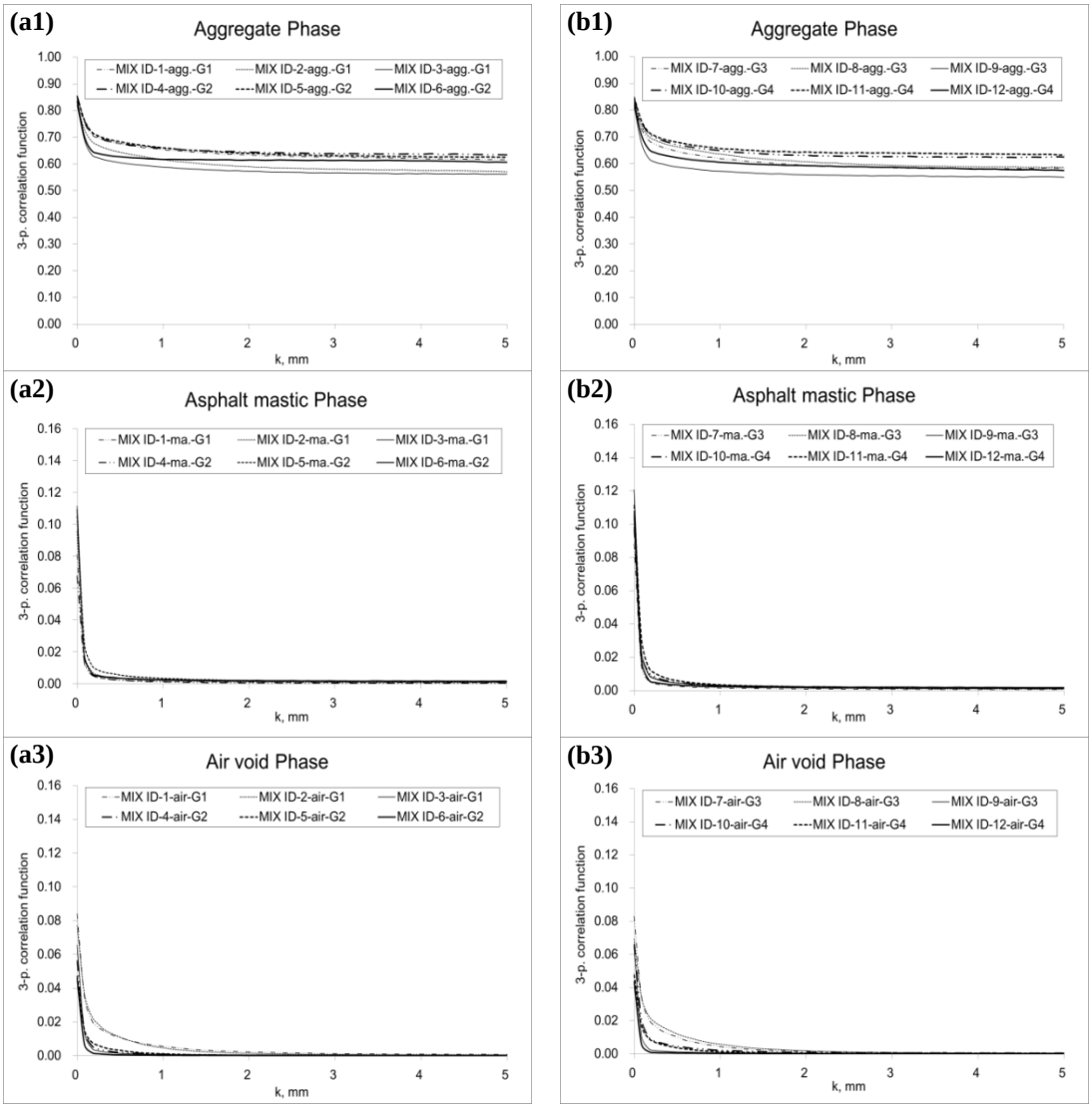

Figure 7: 3-point correlation function for mixture Groups 1 to 4

5.4 Auto Correlation Length (ACL)

Based on the computation results of 2- and 3-point correlation functions, Auto Correlation Length (ACL), which explains how quickly a random event disappears, was calculated. ACL value, which can be also used for estimation of Representative Volume Element (RVE), was calculated as the length of k and l where the estimated values of the function approach to their theoretical values, S^2_1 and S^3_1, respectively within 5% of error level. All the computed results of ACL are shown in Table 6.

From Table 6, it can be first observed that the values of ACL increased with respect to the three phases: aggregate, asphalt mastic and air voids. This means longer computational times are needed for eliminating random events in lower volume fraction components (i.e. asphalt mastic and air voids phases) in comparison with the aggregate phase. Secondly, all the calculated ACL from 7% target air void mixtures showed larger values in comparison with the calculated ACL from 4% target air void mixtures. This is due to different compaction effort used for specimen preparations. Thirdly, RAP mixtures showed higher values of ACL in comparison with the standard mixtures. This indicates larger RVE dimensions for evaluating the mechanical properties of recycled mixtures are needed. In addition, the maximum value of ACL was 4.872mm (Mixture 7) which is smaller than the thickness (=6.35mm) and width (=12.70mm) of BBR creep asphalt specimen. It is worth noting that the Auto Correlation Length (ACL) can be used to measure the distance over which two points can be treated as independent in the specific random process [20]. Based on this property other authors [21] associated the Auto Correlation Length (ACL) with the estimation of the dimensions of the RVE of the material. Therefore, BBR beam can be assumed to be large enough for obtaining the asphalt low temperature creep properties.

Table 6: Auto Correlation Length (ACL) of 2-and 3-point correlation functions

ID	Group	RAP (%)	Air voids (%)	2-point ACL, mm			3-point ACL, mm		
				Agg.	Mas.	Air.	Agg.	Mas.	Air.
1		40		1.302	1.764	3.150	2.782	3.444	3.780
2	1	25	7	0.966	1.386	2.982	2.352	2.772	3.446
3		0		0.798	1.008	1.092	1.512	2.016	2.688
4		40		1.134	1.680	3.066	2.360	2.814	2.940
5	2	25	4	0.882	1.302	2.814	2.184	2.352	2.856
6		0		0.714	0.714	0.882	0.588	1.932	2.016
7		40		1.932	2.142	2.604	2.520	4.872	4.704
8	3	25	7	1.512	1.722	2.436	1.680	3.276	4.368
9		0		0.462	1.218	1.512	0.840	2.520	2.688
10		40		0.924	1.932	2.520	2.100	3.360	4.032
11	4	25	4	0.840	1.680	2.394	1.260	3.108	3.528
12		0		0.294	1.050	1.344	0.504	2.100	2.184

4. CONCLUSIONS

In this paper, the difference in microstructure between conventional and recycled asphalt mixtures was investigated based on spatial distribution information of aggregate, asphalt mastic and air voids phases using advanced 2D DIP analysis technique. Three-phase asphalt images were generated based on volumetric information. It was found that these generated three-phase images can provide more accurate and realistic image of asphalt which indicates these images can be used for generating accurate geometry in FEM and DEM simulation for a follow-up research.

Estimations of 2- and 3-point correlation function were performed on aggregate, asphalt mastic and air voids phases of the generated three-phase asphalt beam images. All the mixtures showed no fluctuations in the 2- and 3-point correlation functions. Based on this result, it can be concluded that the addition of RAP into conventional asphalt up to 40% does not significantly affect the spatial distributions of the material phases even though increase of ACL were observed. Therefore, the significant differences in mechanical performances of RAP mixtures are only partially related to the changes in aggregate, asphalt mastic and air voids spatial distribution in the asphalt mixture.

The images resolution used in this research does not provide an accurate estimation of the fine particles in the asphalt. However, based on this advance DIP technique and on 2- and 3-point correlation function, more detailed microstructure information of asphalt mixtures can be obtained. In addition the proposed analysis procedure may be potentially used by practitioners to evaluate the asphalt in the pavement for forensic controls. The volumetric properties established during mix design can be relatively quickly verified and modification in the mixture preparation may be performed when required.

5. REFERENCES

[1] Recommended Use of reclaimed asphalt pavement in the superpave mix design method: technician's manual, NCHRP report 452, 2001.

[2] Combined 2350/2360 plant mixed asphalt pavement, standard specifications for construction, Minnesota Department of Transportation, 2008.

[3] Effect of reclaimed asphalt pavement (proportion and type) and binder grade on asphalt mixtures, Li X., Marasteanu, M. O., Williams, R. C. and Clyne, T. R., Transportation Research Record, 2051: 90-97, 2008.

[4] Optical methods for the evaluation of asphalt concrete and polymer-modified bituminous binders, Eriksen, K. and Wegan, V., Danish Road Institute, Note 244, 1993.

[5] Prediction of damage behaviors in asphalt materials using a micromechanical finite element model and image analysis, Dai, Q., Sadd, M., Parameswaran, V. and Shukla, A., Journal of Engineering Mechanics, 131(7): 668-677, 2005.

[6] Characterization of air void distribution in asphalt mixes using x-ray computed tomography, Masad, E., Jandhyala, V., Dasgupta, N., Somadevan, N. and Shashidhar, N., Journal of Materials in Civil Engineering, 14(2): 122-129, 2002.

[7] An improved image processing technique for asphalt concrete x-ray CT images, Zelelew, H. M., Almuntashri, A., Agaian, S. and Papagiannakis, A. T., Road Materials and Pavement Design, 14(2): 341-359, 2013.

[8] Modelling of physical properties of composite materials, Torquato, S., International Journal of Solids and Structures, 37: 411-422, 2000.

[9] Microstructural and rheological investigation on the use of recycled asphalt material in asphalt mixtures at low temperature, Cannone Falchetto, A., Montepara, A., Tebaldi, G. and Marasteanu, M. O., Construction and Building Materials, Elsevier, 35: 321-329, 2012.

[10] Recycled asphalt pavement: study of high-rap asphalt mixtures on Minnesota county roads, Johnson, E., Watson, M., Olson, R., Marasteanu, M., Moon, K. H. and Turos, M., Minnesota Department of Transportation, 2013.

[11] Development of a simple test to determine the low temperature creep compliance of asphalt mixture, Marasteanu, M., Velasquez, R., Cannone Falchetto, A., Zofka, A., NCHRP IDEA 133, 2009.
[12] Digital image processing, Gonzalez, R., Prentice-Hall, 2002.
[13] Help documentation, MATLAB R2015a. 2015.
[14] A volumetrics thresholding algorithm for processing asphalt concrete X-ray CT image, Zelelew, H. M. and Papagiannakis, A. T., International Journal of Pavement Engineering, 12(6): 543-551, 2011.
[15] Correlation functions for predicting properties of heterogeneous materials I. Experimental measurements of spatial correlation functions in multiphase solids, Corson, P., Journal of Applied Physics, 45(7): 3159-3170, 1974.
[16] Measurement of spatial correlation functions using image processing techniques, Berryman, J. G., Journal of Applied Physics, 57: 2374-2384, 1985.
[17] Random heterogeneous materials, Torquato, S., Springer-Verlag, New York, 2002.
[18] Modeling heterogeneous materials via two-point correlation functions: Basic principles, Jiao, Y., Stillinger, F. H. and Torquato, S., Physical Review, E76: 031110, 2007.
[19] Investigation of low temperature properties of asphalt mixture containing recycled asphalt materials, Cannone Falchetto, A., Ph.D. Thesis, University of Parma, Italy, 2011.
[20] The effect of autocorrelation length on the real area of contact and friction behavior of rough surfaces, Zhang, Y., Sandararajan, S., Journal of Applied Physics, 97: 103526~103526-7, 2005.
[21] Activation energy based extreme value statistics and size effect in brittle and quasibrittle fracture, Bazant, Z. P. and Pang, S.-D., Journal of the Mechanics and Physics of Solids, 55: 91-134, 2007.